Reaction Ergodography for Unimolecular Decomposition of Ethanol

Tokio Yamabe,*† Masahiko Koizumi, Koichi Yamashita,‡ and Akitomo Tachibana†

Contribution from the Department of Hydrocarbon Chemistry, Faculty of Engineering, Kyoto University, Kyoto 606, Japan. *Received August 3, 1983*

Abstract: Some unimolecular decomposition paths of ethanol were analyzed by ab initio MO calculations in relation to the mode-selective chemical reactions. The geometries and energies of the reactants, transition states, reaction intermediates, and products have been determined for five elementary reaction processes on the singlet potential energy surface of the ground state. The most energetically preferable path is the one for the formation of ethylene. Reaction ergodography along the intrinsic reaction coordinate (IRC) for the decomposition path leading to ethylene clarified two distinct roles of the vibrational modes of ethanol: (1) the vibrational mode excited by the CO_2 laser corresponds to the direction of the reaction path to ethylene and (2) the vibrational mode excited by the HF laser plays a role of energy transfer to the decomposing path to ethylene.

Theoretical chemists have long been interested in a detailed analysis of chemical reaction paths. The chemical reactivity and the reaction dynamics can be well characterized by certain dominant features of the potential energy surface (PES) of chemically reacting systems[1] and especially could be understood by examining these PES characteristics along chemical reaction paths. The analysis of the dynamic aspects of some physical properties along *Fukui's intrinsic reaction coordinate* (IRC),[2] called "reaction ergodography",[3] is one of the most remarkable tools in the theoretical analyses of reaction paths. The IRC, uniquely connecting reactants, transition state (TS), and products, determines the central line of reactive trajectory. Tracing of the IRC therefore shows the very process of chemical change itself. "Reaction ergodography" has been studied on some typical reactions, for example, the substitution and abstraction reaction of methane hydrogens by tritium,[3] the decomposition and isomerization of formaldehyde,[4] some unimolecular reactions of vinylfluoride,[5] the decomposition path of the CH_3NN and CH_3CO radicals,[6] the intramolecular hydrogen rearrangement in formamidine,[7] the double proton exchange in the formamidine–water system,[8] and the isomerization and decomposition of ethyl radical.[9]

Recently laser-induced chemistry[10] has given much interest on the viewpoint of the mode selectivity. The essential problem in this field is what kind of vibrational mode of a reactant is to be initially excited to promote mode-selective reactions.[11] In previous papers we have proposed the idea of vibrational frequency correlation diagrams[4,9] as an example of "reaction ergodography" and analyzed the relation between the vibrational modes and the IRC in the asymptotic region of reactant. The IRC converges at the reactant to the normal mode which initiates the reaction, so this approach would be promising to interpret the laser-induced mechanism.

In this paper we study the laser-induced unimolecular decomposition of ethanol theoretically. It is well-known that ethanol thermally decomposes to give unsaturated compounds or C_1 compounds by a radical chain mechanism.[12] Recently it has been reported, however, that the following unimolecular decompositions of ethanol could be controlled by laser.

$$CH_3CH_2OH \rightarrow CH_2{=}CH_2 + H_2O \quad \text{(process I)}$$

$$CH_3CH_2OH \rightarrow CH_3CHO + H_2 \quad \text{(process II)}$$

$$CH_3CH_2OH \rightarrow CH_3 + CH_2OH \quad \text{(process III)}$$

In the experiment by a pulsed HF laser (3644 cm^{-1}),[13] process I proceeds preferentially under a low-pressure condition. Above 10 torr, the increase of the products of the three reactions is proportional to the ethanol pressure, maintaining the ratio II:I:III = 3:2:1 approximately. On the other hand, a pulsed CO_2 laser (1039 cm^{-1})[14] induces specifically process I. In order to clarify this characteristic selectivity, we investigate the ground-state singlet PES of ethanol by ab initio MO calculations and perform "reaction ergodography" to explain the role of the vibrational modes of ethanol in the laser-induced elementary reaction processes I and II.

Scheme I

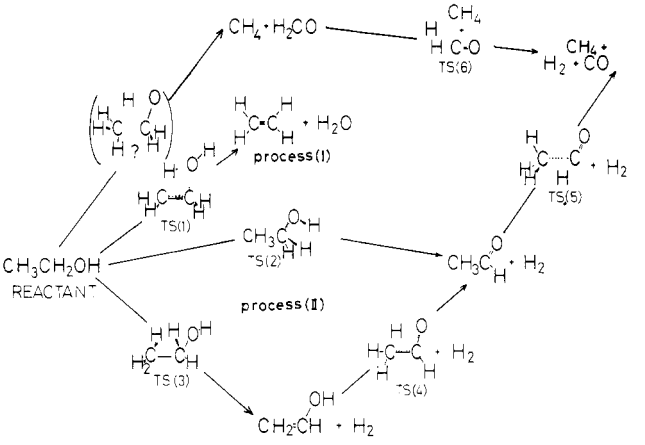

Reaction Mechanism Models

Scheme I shows the mechanisms of the possible elementary processes considered in this paper. The mechanism by which ethanol loses H_2O through the four-center transition state TS(1), which possesses a newly bonded O–H, H of the methyl group,

†Division of Molecular Engineering, Graduate School of Engineering, Kyoto University, Kyoto 606, Japan.

‡Present address: Department of Chemistry, University of California, Berkeley, CA 94720.

(1) (a) R. B. Woodward and R. Hoffmann, *Angew. Chem., Int. Ed. Engl.*, **8**, 781 (1969); (b) J. C. Polanyi, *Acc. Chem. Res.*, **5**, 161 (1972).
(2) (a) K. Fukui, *J. Phys. Chem.*, **74**, 4161 (1970); (b) K. Fukui, S. Kato, and H. Fujimoto, *J. Am. Chem. Soc.*, **97**, 1 (1975); (c) K. Ishida, K. Morokuma, and A. Komornicki, *J. Chem. Phys.*, **66**, 2153 (1977).
(3) S. Kato and K. Fukui, *J. Am. Chem. Soc.*, **198**, 6395 (1976).
(4) K. Yamashita, T. Yamabe, and K. Fukui, *Chem. Phys. Lett.*, **84**, 123 (1981).
(5) S. Kato and K. Morokuma, *J. Chem. Phys.*, **74**, 6268 (1981).
(6) K. Yamashita, M. Kaminoyama, T. Yamabe, and K. Fukui, *Chem. Phys. Lett.*, **83**, 78 (1981).
(7) K. Yamashita, M. Kaminoyama, T. Yamabe, and K. Fukui, *Theor. Chim. Acta*, **60**, 303 (1981).
(8) T. Yamabe, K. Yamashita, M. Kaminoyama, M. Koizumi, A. Tachibana, and K. Fukui, *J. Phys. Chem.*, in press.
(9) (a) K. Yamashita, T. Yamabe, and K. Fukui, *Theor. Chim. Acta*, **60**, 523 (1982). (b) K. Yamashita, T. Yamabe, and K. Fukui, *J. Am. Chem. Soc.*, submitted for publication.
(10) R. N. Zare and R. B. Bernstein, *Phys. Today*, **33**, 43 (1980).
(11) (a) N. Bloembergen and E. Yablonovitch, *Phys. Today*, **33**, 83 (1980); (b) "Advancement in Laser Chemistry", A. H. Zeweil, Ed., Springer, New York, 1978; (c) "Laser-Induced Process in Molecules", K. L. Kompa and S. D. Smith, Eds., Springer, New York, 1979.
(12) J. A. Bernard and H. W. D. Hughes, *Trans. Faraday Soc.*, **56**, 55 (1960).
(13) L. Selwyn, R. A. Back, and C. Willis, *Chem. Phys.*, **36**, 323 (1978).
(14) Wayne C. Danen, *J. Am. Chem. Soc.*, **101**, 1188 (1979).

0002-7863/84/1506-2255$01.50/0

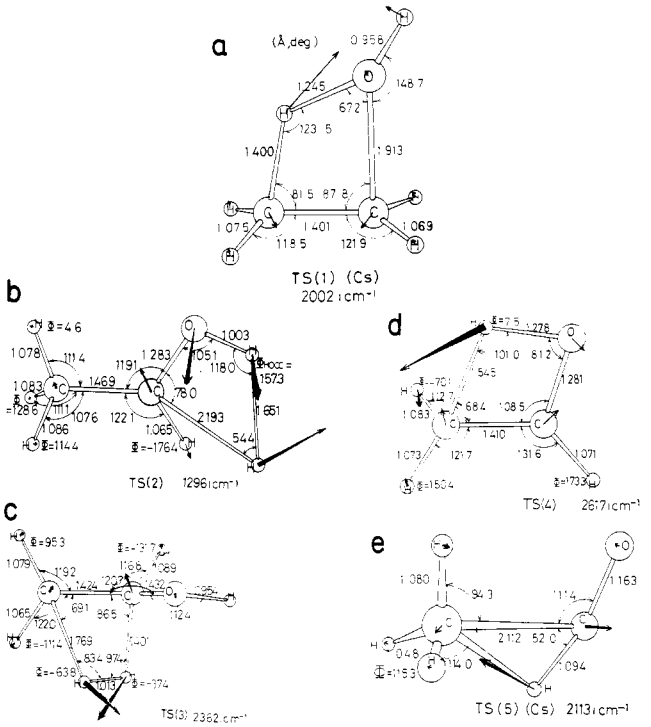

Figure 1. Optimized geometries and displacement vectors of the reaction coordinate for transition states. Φ is a dihedral angle ∠HCCO.

is assigned to elementary process I. For process II, two kinds of mechanisms are considered. One is the one-step elimination mechanism which provides acetaldehyde and H_2 directly through TS(2). The other mechanism is the two-step one which includes the elimination of H_2 from neighboring carbons to form vinyl alcohol, CH_2=CHOH, through TS(3) and a subsequent H-migration of the intermediate (CH_2=CHOH) yielding CH_3CHO through TS(4). Moreover we propose the process that CH_3CHO dissociates to CH_4 and CO through the three-center structure of TS(5).

Method of Calculations

We used a GAUSSIAN 80[15] program package for the following MO calculations with the split-valence 4-31G basis set.[16] The geometries of equilibrium points were optimized by the energy gradient method.[17]

We performed the configuration interaction (CI) calculations[18] in order to obtain more reliable energy estimates at the 4-31G optimized geometry in processes I and II. All the single and double excitations from the HF reference configuration were included in the CI wave functions, with the 1s orbitals of carbon and oxygen kept fully occupied. In addition, the contribution of unlinked quadruple excitations was estimated with Davidson's formula[19]: $(1 - C_0^2)\Delta E_{sd}$, where C_0 is the coefficient of the HF configuration and ΔE_{sd} is the correlation energy coming from the single and double excitations.

The vibrational analysis and the tracing of the IRC are carried out by using the HONDO[20] program. The second derivatives of the PES required for the vibrational analysis at some optimized geometries are obtained by the numerical differentiation of the analytically calculated energy gradient.[17]

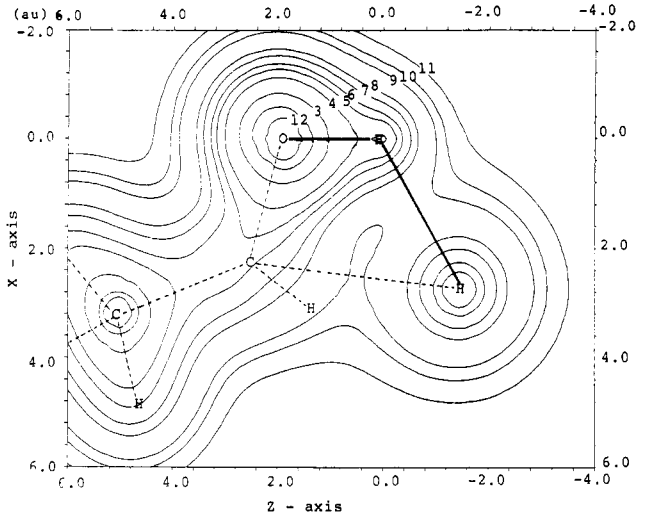

Figure 2. Density map of TS(2). The *XZ*-plane includes the oxygen and the two leaving hydrogen atoms. The numbers 1–11 on contours correspond to the values (au) 3.0, 1.0, 0.6, 0.3, 0.2, 0.15, 0.1, 0.07, 0.03, 0.02, and 0.01, respectively.

The statistical *A*-factors of processes I and II are estimated by the simplified transition-state (TS) theory[21] expression

$$A_\infty = \frac{\nu_1\nu_2\cdots\nu_n}{\nu_1^*\nu_2^*\cdots\nu_{n-1}^*}$$

where ν_i and ν_i^* are the reactant and TS vibrational frequencies, respectively.

Results and Discussion

(1) Structures and Vibrational Modes of the Transition States. The fully optimized geometries of TS(1)–(5) and the displacement vectors of normal modes with imaginary frequency are shown in Figure 1. These vectors provide the initial direction of the IRC leading to the products.

The structure of TS(1) for process I has the C_s symmetry. The decomposing C–O and C–H bond lengths are 30% larger than that of the reactant, and the newly formed O–H bond length (1.245 Å) is close to that of the water molecule produced. The displacement vector well represents the elimination of HOH from the ethylene part.

As for TS(2), the C–O bond length (1.283 Å) is closer rather to that of the reactant ethanol than to the carbonyl bond length of the product acetaldehyde. The decomposing C–H bond length is twice as long as that of the reactant, and the Mulliken overlap population (0.041) between these two atoms shows that this bond is almost cleaved. In contrast with this, however, the decomposing O–H bond length (1.003 Å) stretches by only 5%. The displacement vector at TS(2) shows that the movement of the O atom is large as well as that of both H atoms. Interestingly, it is noted that the H atom leaving from the C atom is anionic while the other H atom leaving from the O atom is cationic. This trend may be attributed to the long C–H bond length at TS(2). This characteristic localization of electron is represented well by the electron distribution map in Figure 2. The distribution of electron density is localized on the O atom and the H atom leaving from the C atom. On the contrary, the density on the H atom leaving from the O atom is small. The net charges of these atoms are −0.630 on the O atom, −0.602 on the H atom leaving from the C atom, and +0.420 on the H atom leaving from the O atom, respectively.

For TS(3) producing vinyl alcohol, the difference of the degree of stretching between two cleaving C–H bond lengths is large as shown in Figure 1c. One C–H bond length increases by 60%, the

(15) (a) J. S. Binkley, P. C. Hariharan, R. Seeger, J. A. Pople, and M. D. Newton, *QCPE*, **13**, 368 (1981); (b) J. A. Pople et al., *ibid.*, **13**, 406 (1981).
(16) R. Ditchfield, W. J. Hehre, and J. A. Pople, *J. Chem. Phys.*, **54**, 724 (1971).
(17) P. Pulay in "Modern Theoretical Chemistry", H. F. Schaefer, Ed., Plenum, New York, 1977, Vol. 4.
(18) B. D. Roos and P. Siegbahn in "Methods of Electronic Structure Theory", H. F. Schaerfer, Ed., Plenum, New York, 1977, Chapter 7. We used the direct CI program in the Alchemy system (M. Yoshimine, A. P. McLean, B. Liu, M. Dupuis, and P. S. Bagus, National Resource Computer Chemistry Software Catalog, No. 1, Program No. QC03 (1980)).
(19) E. R. Davidson and D. W. Silver, *Chem. Phys. Lett.*, **52**, 403 (1977).
(20) M. Dupuis and H. F. King, *J. Chem. Phys.*, **68**, 3998 (1978).
(21) P. J. Robinson and K. A. Holbrook, "Unimolecular Reactions", Wiley, New York, 1972.

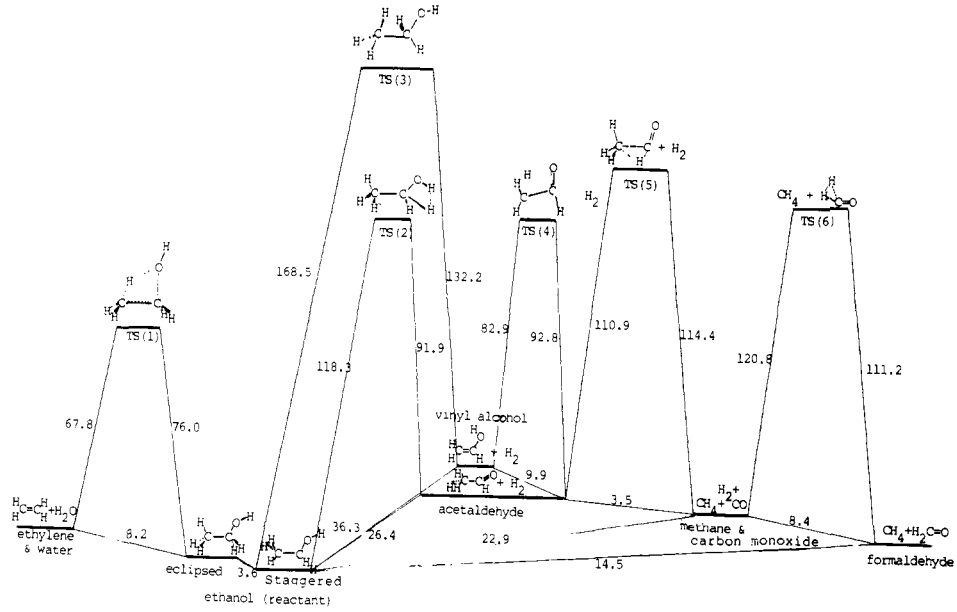

Figure 3. Energy diagram illustrating unimolecular reaction of CH_3CH_2OH. Energies (kcal/mol) are calculated by using the 4-31G optimized geometry.

other one by 30%. In contrast with the case of TS(2), however, neither of the two H atoms shows ionic character.

In the process of the isomerization from vinylalcohol to acetaldehyde, L. Radom et al.[22] have already determined, in the STO-3G level of calculation, the favorable TS with the four-center structure. We have obtained a similar structure of TS(4) as shown in Figure 1d, where the migrating hydrogen is almost on the CCO plane corresponding to the fact that the antarafacial migration is symmetry allowed for the 1,3-sigmatropic shift. The displacement vector shows the dominant motion of the migrating hydrogen atom.

For the C–C cleavage of acetaldehyde accompanied by the migration of the carbonyl hydrogen atom producing methane and carbon monoxide, we determined TS(5) within the C_s symmetry. The breaking C–C bond length stretches by 40% from the acetaldehyde, but the length of the C–H bond on carbonyl site does not change so remarkably. The displacement vector shows that the migrating H atom approaches the methyl group rapidly after passing TS(5).

(2) Potential Energy Surfaces and Reaction Mechanisms. The energy diagram of the elementary processes I and II are schematically presented in Figure 3.

The E_a (activation energy) value of TS(1) for the formation of ethylene is calculated to be 76.0 kcal/mol. The E_a's for the processes which produce CH_3CHO, either the direct eliminative mechanism via TS(2) or the two-step eliminative mechanism through the CH_2=CHOH intermediate, are calculated to be larger than 100 kcal/mol. E_a of process III, for which calculations are not carried out in this study, is estimated to be 89 kcal/mol from experimental data.[13] Therefore the elementary process I is considered to be the most preferable path energetically in unimolecular processes.

In process II producing acetaldehyde, the one-step mechanism via TS(2) is more favorable than the two-step mechanism via TS(3), vinylalcohol, and TS(4).

In order to estimate the E_a's for process I and the one-step process of II more accurately, the CI calculations are carried out. As mentioned before, TS(2) for the one-step process of II has a very localized nature of electron distribution, so this energy height might be reduced by the CI calculations. Table I shows the E_a's obtained by the CI calculations and with quadruple corrections (QC). Both the E_a's of TS(1) for process I and TS(2) for the one-step process of II are reduced by 6–7 kcal/mol on the CI + QC level. The former E_a value (72.6 kcal/mol) is in good agreement with the experimental value (71 kcal/mol) by Danen.[14] The E_a's of process II are still higher than those of process I.

Table I. Calculated Relative Energies (kcal/mol) with the 4-31G Basis Set

		S + D[a]	
	SCF	CI[b]	CI + QC[c]
reactant (staggered)	0	0	0
TS(1)	79.6	74.5	72.1
TS(2)	118.3	114.5	112.1

[a] Single and double excitations. [b] Configuration interaction calculations. [c] CI calculations with quadruple corrections.

Table II. *A* Factor for Processes I and II

reaction	$(10^{-14})A$ factor, s^{-1}
$CH_3CH_2OH \rightarrow$ TS(1)	1.733
$CH_3CH_2OH \rightarrow$ TS(2)	3.084
$CH_3CH_2OH \rightarrow$ TS(3)	3.928

The second factor to be considered is the frequency factor (A-factor) for each process. The values calculated are in Table II and show that the A-factor of process II is twice as large as that of process I. Thus process II is considered to be more favorable than process I in terms of the entropy factor. But in such a temperature region as adopted by the experiment, this entropy factor may not be so important.

Both the Arrhenius parameters calculated in this study explain well the experimental result that the dominant products are ethylene and water through process I under low-pressure conditions. In the lower pressure region, the lasers play a role of an energy pump to heat the reactant molecule.

If the pressure becomes higher, this unimolecular decomposition process may be disturbed because of the more frequent intermolecular collisions. the intermolecular V–V or V–T energy transfers distribute the vibrational energy which was originally stored in each molecule by the laser excitation. It follows that the formation of ethylene is inhibited. This mechanism explains well the low-pressure results of experiment.[13] Therefore, in the higher pressure region, a more complex process might appear.

As for process I, the quantum yield at the lower pressure region is remarkably large. This shows that the HF laser plays an important role of activating the reactant molecule. Moreover, at the higher pressure region, the quantum yield for process I is quite large when compared with the thermal experiment. This implies that the HF laser may easily produce the activated species

(22) W. J. Bouma, D. Poppinger, and L. Radom, *J. Am. Chem. Soc.*, **99**, 6443 (1977).

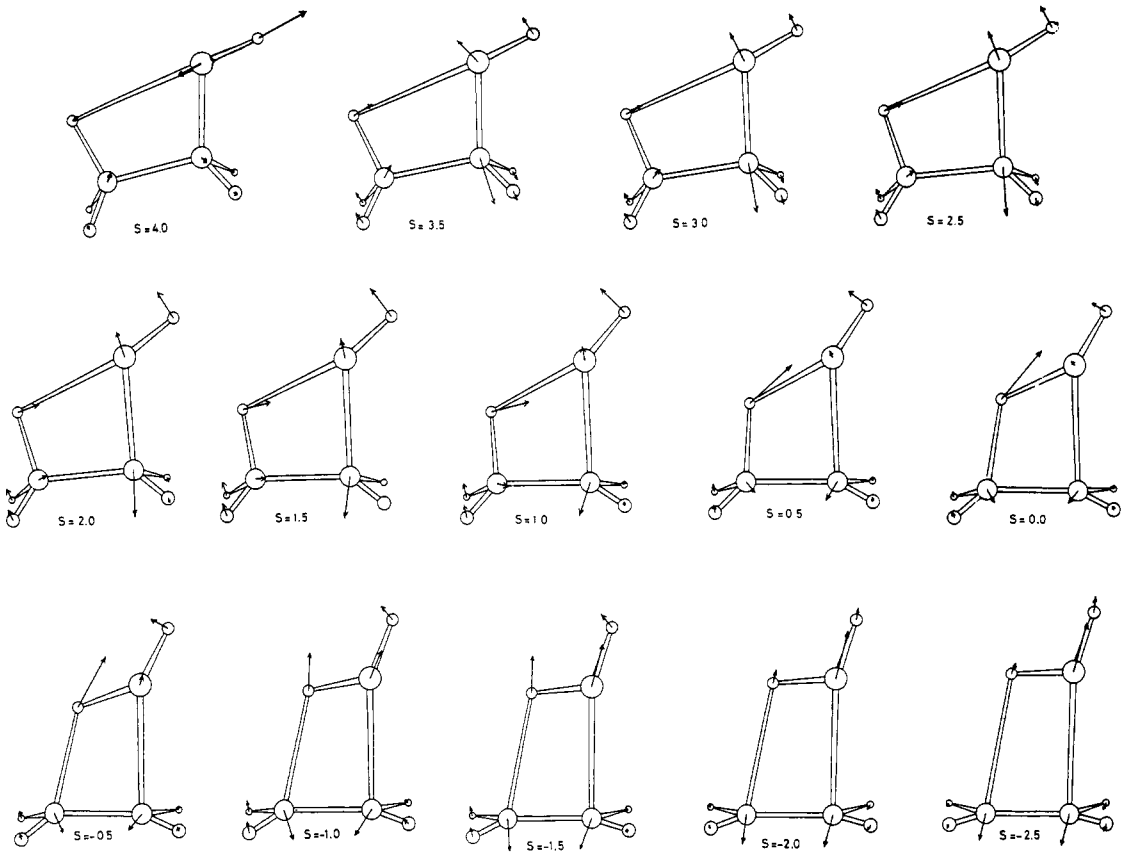

Figure 4. Change of nuclear configuration and displacement vector in process I.

leading to ethylene even under higher pressure condition. The precise mechanism of the laser action will be discussed in section 4.

As for process II, the quantum yield at the lowest pressure region is overwhelmingly small compared with that of process I. This is explained well by the energy diagram of Figure 3. The high E_a's of process II are responsible for the small yield of reaction. Moreover, even if the acetaldehyde is produced by process II, the formation of carbon monoxide is difficult because the E_a through TS(5) is very large. This corresponds to the experimental result that the carbon monoxide was below limit of detection.[13]

In process III the breaking of the C–C bond does not so easily occur by excitation of the O–H bond stretching mode; furthermore this E_a for the cleavage of the C–C bond obtained by the experiment[13] is much higher than the E_a of TS(1) but is lower than that of TS(2). Therefore, the amount of the species produced by this process (III) is expected to be smaller than that of process I and larger than that of process II. This is in good agreement with the lower pressure result of the HF laser experiment.[13]

(3) Analyses of Intrinsic Reaction Coordinate (IRC). In this section we analyze the IRC's for the elementary process I and the one-step elementary process of II, for comparison. The difference in the role of the vibrational modes of ethanol in the mode-selective reactions by CO_2 laser and HF laser will be discussed in section 4.

Figures 4 and 5 show the graphical geometry changes of the reactant molecule for each process, respectively, s is the length measured along the IRC on the PES, and the unit of s is (atomic mass unit)$^{1/2}$ (bohr). The TS is located at $s = 0.0$, and the plus sign of s indicates the reactant region of the reaction. Therefore the reaction is considered to proceed by reducing the s value and by passing through the TS at $s = 0.0$.

In Figure 6, we show the changes of the potential energy (PE), the norm of the energy gradient (N_g), the main bond lengths and the bond angles along the IRC's for the processes I, and the one-step process of II. Two processes proceed from center to both sides, respectively.

Since TS(1) of process I has C_s symmetry, we assume that the IRC conserves this symmetry. In the early stage of process I (s = 4.0–1.0), the O atom moves drawing an arc on the molecular plane and stretching the CO bond length. The removing H atom of the CH_3 group begins to move rapidly from the point at s = 0.5 in the vicinity of TS(1) where the N_g is maximum, and the new bonding formed between this H atom and the O atom. A large imaginary vibrational frequency 2002i cm^{-1} of TS(1) means that a sudden change of the PE occurs around the TS(1). The largeness of the E_a on the removal of H from the CH_3 group may mainly contribute to this sudden change.

On the other hand, in the one-step process of II, the C–H bond of the CH_2 group stretches and the OCH angle contracts rapidly from the beginning. N_g becomes maximum already around s = 2.3, the neighborhood of the reactant, and the change of PE is remarkably small in the early stage of the reaction, contrary to process I. The E_a for the removal of H from the CH_2 group largely contributes to this early change of PE. The leaving H on the O site begins to move near TS(2), and at this point the C–H bond has already stretched. The PE change near TS(2) is not as rapid as that of process I. This fact corresponds to the small imaginary vibrational frequency, 1290i cm^{-1}. In other words, the elimination of the H atom from the OH group is characterized by the moderate change of PE. This is explained by the electronic structure in the neighborhood of TS(2) as described in section 1 of Results and Discussion that the almost free hydride ion attached to carbon abstracts a proton from the OH group and produces stable hydrogen molecule.

(4) Reaction Selectivity by Laser. In this section, we try to explain the role of the vibrational modes of the reactant in the reaction selectivity of the experiment by using a laser. Essential to this problem is what kind of vibrational mode of a reactant molecule is excited initially and how the reaction pathway interacts with the excited vibrational mode.

Some of our previous works[4,9] have clarified the relation between the vibrational modes and the IRC in the asymptotic region of the reactant, and the role of the vibrational modes are summarized as follows.

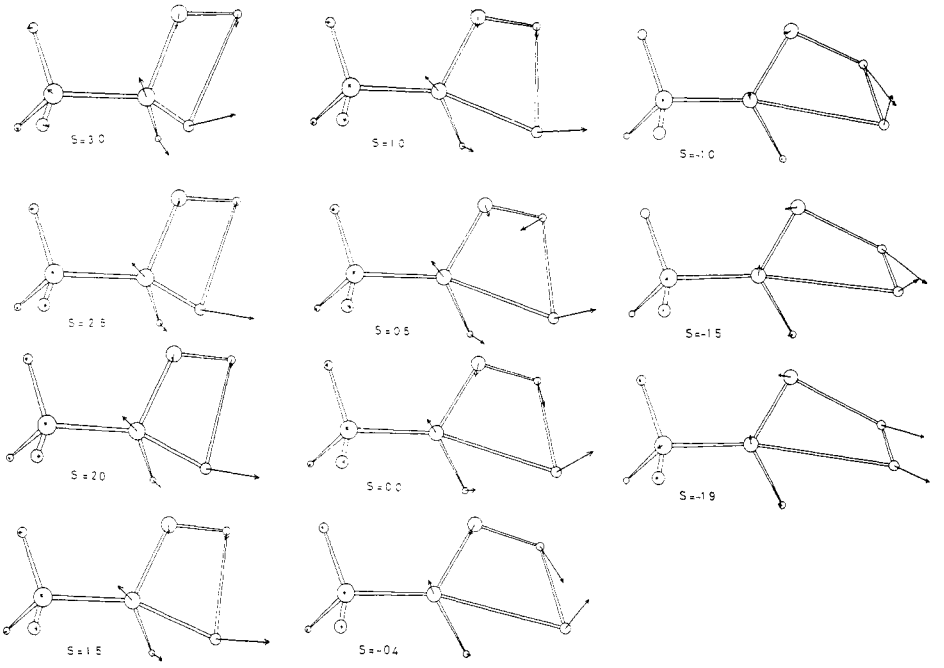

Figure 5. Change of nuclear configuration and displacement vector in process II.

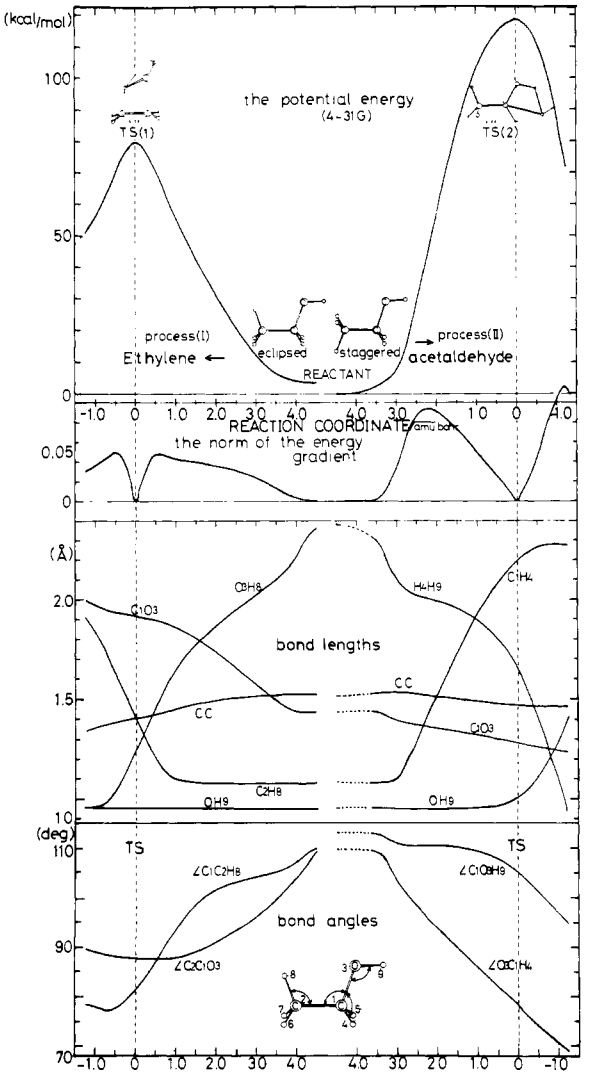

Figure 6. IRC analysis of processes I and II.

The dynamic aspects of a reacting system are well described by the coupling between the IRC and the vibrational modes perpendicular to the IRC. Some vibrational modes are strongly coupled with the IRC, and these strongly coupled modes twist the IRC in the configuration space. In the relation between the twisting of the IRC and the location of the barrier (1) the excitation of the vibrational mode to which the IRC converged at the reactant is most effective for a channel where the IRC twists after the TS (the late twisting the IRC) and (2) the excitation of a strongly coupled mode is most effective for a channel where the IRC twists before the TS (the early twisting the IRC). Another type of vibrational mode plays a part of energy supply mode. The vibrational energy pumped in this mode by laser is transferred to the particular mode mentioned above. A mechanism of this intramolecular vibrational energy transfer is determined by the mode coupling between the vibrational modes along the IRC.

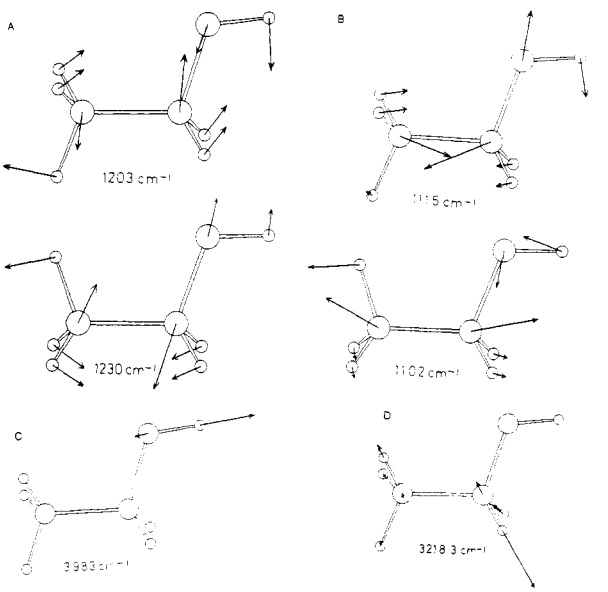

Figure 7. Main vibrational normal mode of reactant (ethanol): (A) CO stretching mode; (B) asymmetric CCO stretching mode; (C) OH stretching mode; (D) asymmetric CH_2 stretching mode.

Figure 7 shows the main normal vibrational modes of the reactant (ethanol). It is well accepted that the ordering of vibrational frequencies are well reproduced in our level of calculations and that the experimental frequencies would be obtained by a reduction of 10–15% from the calculated ones.[17]

Therefore it is considered that a CO_2 laser (1039 cm^{-1}) will excite the CO stretching mode (1203 cm^{-1}, calculated value of the staggered form; see Figure 7A) or the asymmetric CCO stretching mode (1115 cm^{-1}; see Figure 7B). It is noted that the displacement vectors of these modes correspond to the initial direction of the IRC of process I, where the CO stretching and the CCO angle contracting is remarkable in the early stage of the reaction. Therefore, a CO_2 laser excites the vibrational mode which corresponds to the direction of the reaction path and induces process I selectively.

On the other hand, the HF laser (3644 cm^{-1}) is considered to excite the OH stretching mode (3983 cm^{-1}; see Figure 7C) of ethanol. In the one-step process of II, however, the deformation of the reactant molecule has no contribution of the OH stretching along the IRC. Therefore, the OH stretching mode excited by the HF laser does not play a part as a direct mode to deform the molecule to the direction of the IRC of the one-step process of II. The OH stretching mode interacts with the IRC of process I better than that of the one-step process of II. Because in the reactant region (s = 4.0) the displacement vector of the reactant has the component of the OH stretching and the symmetry of the OH stretching mode is C_s, the vibrational energy transfer to the CCO deformation or the asymmetric CCO stretching modes which is expected to interact with the IRC of process I is more effective than that to the asymmetric CH_2 stretching mode (3218 cm^{-1}; see Figure 7D) which is expected to interact with the IRC of the one-step process of II.

Therefore it is considered that the energy supplied by HF laser is effectively used to promote the unimolecular rate process I. This explains well the HF laser enhancement of process I under the condition of low pressure.[13]

Conclusion

In this study we investigated the reaction paths of the unimolecular decomposition of ethanol especially in connection with the mode-selective chemical reactions.

Five unimolecular decomposition paths were analyzed by ab initio MO calculations. The geometries and energies of the reactants, TS's, reaction intermediates, and products have been determined on the singlet PES. The most energetically favorable unimolecular path is the formation of ethylene. With respect to the acetaldehyde formation, the one-step mechanism is more favorable than the two-step mechanism via vinylalcohol. A possible radical formation process is also suggested.

We also discussed the dissociation paths leading to ethylene or acetaldehyde on the basis of "reaction ergodography". We found that the CO stretching or asymmetric CCO stretching modes which would be excited by CO_2 laser correspond to the displacement vector of the IRC for the decomposition to ethylene, so that CO_2 laser highly selects the reaction path to ethylene. Moreover the OH stretching mode excited by HF laser plays a role of energy transfer to the reaction path leading to ethylene.

Acknowledgment. The numerical calculations were carried out at the Data Processing Center of Kyoto University and the Computer Center of Institute for Molecular Science (IMS).

Registry No. Ethanol, 64-17-5.

Microwave Spectroscopic Study of Malonaldehyde. 3. Vibration–Rotation Interaction and One-Dimensional Model for Proton Tunneling

Steven L. Baughcum,[1a] Zuzana Smith, E. Bright Wilson,* and Richard W. Duerst[1b]

Contribution from the Department of Chemistry, Harvard University, Cambridge, Massachusetts 02138. *Received November 18, 1983*

Abstract: Strong perturbations are observed in the microwave spectra of a number of isotopically substituted species of malonaldehyde, all containing deuterium in the hydrogen bond. They are well fitted by using Pickett's reduced axis system (RAS) for the definition of the rotating axes. (Instantaneous principal axes do not fit the data as well and are much less convenient.) The RAS fit gives accurate values for the rate of deuterium transfer between the two oxygen atoms in eight symmetrically substituted isotopic species and in two unsymmetrically substituted species, namely ($D_6D_8{}^{13}C_{2-4}$) and ($D_6D_8{}^{13}C_{2-4}{}^{13}C_3$). The inverse cross product of inertia, F, is also obtained from the fit. An attempt to put rough limits on the height (V_b) and width ($2x_o$) of the barrier separating the two equivalent potential minima was only moderately successful, the barrier height for deuterium tunneling species lying in the range 4.0–5.2 kcal/mol and the separation of the two minima ranging from 0.994 to 0.822 Å for the various isotopic species, as determined from the earlier microwave structure. The effective mass to be used with the pseudo-one-dimensional double-minimum potential function was estimated to be ~1.2 au for the parent species and 2.12 to 2.53 au for the several species with deuterium tunneling. These values were estimated from the experimental values of the ab cross term $\langle 0|F|1\rangle$ in the inverse tensor and the tunneling splittings. An alternative approach used the slightly differing tunneling splittings, ΔE_{01}, for a set of symmetrically isotopically substituted species. This latter approach yields also the contribution of each atom to the effective mass. The results indicate that the reaction path near the transition state deviates only a little from parallelism to x_6, the a component of the displacement of the proton in the H bond.

Malonaldehyde (3-hydroxy-2-propenal, see Figure 1) is one of the simplest molecules containing a ring closed by a hydrogen bond. It should therefore be a suitable system to investigate in order to extract information about the forces acting in this bond both from the analysis of spectroscopic data and from quantum chemical calculations of various levels levels of approximation.

In the vapor phase, the two equivalent unsymmetrical planar equilbrium configurations shown in Figure 1 have been demonstrated to be present.[2,3] Rapid tunneling occurs between these

(1) (a) Present address: Los Alamos National Laboratory, Los Alamos, NM 87545. (b) Present address: Analytical and Properties Laboratory, 3M Center, St. Paul, NM 55144.

(2) (a) Rowe, W. F., Jr. Ph.D. Thesis, Harvard University, 1975. (b) Baughcum, S. L. Ph.D. Thesis, Harvard University, 1978.

0002-7863/84/1506-2260$01.50/0